DESIGN OF A SPACE-BORNE HYPERSPECTRAL IMAGER FOR MICRO-SATELLITES

Zeynep Nilüfer Öztürk[1,2], Mustafa Ekinci[1], Özgür Karcı[3]

[1] Tübitak Space Technologies Research Institute, Ankara, Türkiye (nilufer.ozturk, mustafa.ekinci@tubitak.gov.tr)
[2] Middle East Technical University, Physics Department, Ankara, Türkiye (e160432@metu.edu.tr)
[3]Turkish Aerospace Industry, Ankara, Türkiye (ozgur.karci@tai.com.tr)

KEYWORDS: Space-borne hyperspectral imagers, earth observation, three mirror anastigmat, imaging spectroscopy, remote sensing

ABSTRACT:

We present an optical design of a space-borne hyperspectral imager (HSI) for Earth observation micro-satellite platforms. Space-borne hyperspectral imaging has many crucial applications in fields such as agriculture, water management, environmental monitoring, mineralogy, and remote sensing. An HSI system capable of ground sampling distance (GSD) less than 15 m with a swath width greater than 15 km, spectral resolution less than 10 nm and operating in Low Earth Orbit (LEO) is designed. The system dimensions are restricted to fit in a volume of less than 0.125 m^3. A commercial, cooled HgCdTe type imaging sensor is selected to operate 400 – 2500 nm of the spectrum for the designed imager. The HSI optical design comprises of an off-axis three mirror anastigmat (TMA) type telescope and a modified-Offner type spectrometer. Modified-Offner type spectrometer design with two Féry prisms as a diffractive element is used. The overall HSI system design meets the performance goals described in this paper work.

1. INTRODUCTION

Hyperspectral space-borne imaging was introduced in the late 1980s for airborne mineral mapping by Goetz (Eismann, 2012). Hyperspectral imaging is a fast-growing and promising area of remote sensing, combining two main remote sensing techniques which are imaging and spectroscopy. Hyperspectral imagers allow for capturing of images with much higher spectral resolution than traditional multispectral cameras that capture images in the red, green, blue (RGB) and NIR spectrum. They collect images across a broad spectrum of wavelength, typically including the visible and near-infrared (NIR) or shortwave infrared (SWIR) spectrum. One of the main advantages of hyperspectral imaging is its ability to capture detailed spectral information from a scene. This allows researchers to identify and distinguish between different materials based on their unique spectral signatures. For example, in agriculture, HSIs can be used to identify the health and growth of crops by detecting subtle changes in chlorophyll content and soil moisture levels. In geology, these imagers can help identify minerals or other materials based on their reflectance spectra. However, the technology is still relatively expensive and requires specialized training to operate and analyse data effectively. Nonetheless, advancements in sensor design and data analysis algorithms are making hyperspectral imaging more accessible and practical for a growing number of research and industrial applications. The demands of hyperspectral imaging for Earth's surface, atmosphere observation, and environmental monitoring applications from space push the limits of the telescopes and imaging sensors forward.

Numerous hyperspectral designs have been studied in literature. Optical system parameters of published HSI designs, which have similar requirements with this study are shown and compared in Table 1. Some of the published HSI designs are investigated at this part of the paper. Hyperion is a hyperspectral imager designed and built by NASA (Calin et al. , 2021). The HSI instrument is mounted on the Earth Observing-1 (EO-1) satellite to operate in LEO orbit, which was launched in 2000. Hyperion captures images with a swath width of 7.7 km. The Compact High-Resolution Imaging Spectrometer (CHRIS) is a hyperspectral imager developed by the European Space Agency (ESA) (Escalante-Ramírez et al., 2012). It was launched in 2001 on board the PROBA-1 satellite and is still in operation in LEO orbit today. One of the key advantages of the CHRIS hyperspectral imager is its high spatial resolution. The Advanced Responsive Tactically Effective Military Imaging Spectrometer (ARTEMIS) is a hyperspectral imager designed for remote sensing applications (Qian, 2021). The ARTEMIS, an advanced hyperspectral imager, was included in the TacSat-3 satellite, which was launched in 2009. The ARTEMIS hyperspectral imager used a single 2-D HgCdTe detector array that covered both VNIR and SWIR spectral regions, providing a 4 km swath width. The Hyperspectral Environment and Resource Observer (HERO) is an HSI designed by Canadian Space Agency (CSA) (Bergeron et al., 2008). The HERO is planned as an operational hyperspectral mission capable of covering an area of more than 600,000 km^2 daily. The resulting image consists of radiance spectra that can be transformed into reflectance spectra by correction of the influence of the atmosphere. The total instrument MTF is at least 0.3 at Nyquist frequency at all wavelengths and fields. The smile and keystone distortions are less than 10%. The Copernicus Hyperspectral Imaging Mission for the Environment (CHIME) (Celesti et al., 2022) is a satellite mission designed to provide detailed imaging of the Earth's surface using hyperspectral technology. The mission is being developed by ESA and is part of the European Union's Copernicus program. The HSI instrument has a spectral resolution of 10 nanometers and is able to image in over 200 bands over a wavelength range from 400 nm - 2500 nm in the visible (VIS), near infrared (NIR), and short-wave infrared (SWIR) spectrum. CHIME HSI will be able to measure at a ground resolution of 30 m for a swath width of 130 km and will operate in LEO orbit. CHIME is planned to be launched in 2028.

Parameter	Hyperion	Chris	Hero	HSI
Telescope Design	TMA	Two-mirror	TMA	TMA
Spectrometer Design	Offner	Modified Offner	Offner Dyson	Modified Offner
Effective Focal Length	1320 mm	746 mm	704 mm	712 mm
Aperture Diameter	120 mm	120 mm	320 mm	200 mm
GSD	30 m	17 m	30 m	14.7 m
Altitude	705 km	700 km	700 km	700 km
Spectral Resolution	10 nm	1.25 nm	7.5 nm	8.3 nm
Bandwidth	400-2500 nm	400-1050 nm	400-2500 nm	400-2500 nm

Table 1. Comparison of HSI design parameters

The HSI design presented in this study is aimed for environmental monitoring applications. The resulting design is restricted to fit in a volume less than 0.2 m^3 to be used in a micro-satellite platform. Our study showed that, it is not possible to optimize the system with standard mirror surface forms according to the performance goals of the design in a compact volume for micro-satellite platforms. Therefore, even aspheric surface forms need to be defined in the design to fit in compact volume. In this paper, all the system engineering calculations and each parameter of HSI design are investigated in detail.

2. SYSTEM OVERVIEW

Performance goals of the project are shown in Table 2. Imaging sensors should also be decided according to the performance goals before the optical design process. The imaging sensor is chosen due to three main parameters: cost, availability, and performance. In Table 3 chosen sensor parameters are shown.

Parameter	Value
Orbital Altitude *(H)*	700 km [LEO orbit]
Image Scanning Technique	Push-broom
Ground Sampling Distance *(GSD)*	≤ 15m
Spectral Resolution	≤ 10 nm
Swath Width	>15 km
Wavelength Range	400-2500 nm
Spatial Distortion (Smile)	≤ 15 µm
On-ground pixel smile	1.5 m
Spectral Distortion (Keystone)	≤ 15 µm
Modulation Transfer Function (MTF)	≥36

Table 2. Performance goals of the hyperspectral imager

Parameter	Value
Pixel Size	15 x 15 µm
Number of pixels	1024 x 256
Number of spectral pixels *(#sp)*	256
Number of spatial pixels *(#stp)*	1024
Bandwidth	400-2500 nm
Detector	HgCdTe
Scanning sensor type	Push-broom

Table 3. Specifications of a customized imaging sensor

3. THEORETICAL BACKGROUND OF THE SYSTEM DESIGN PARAMETER CALCULATIONS

Optical system design parameter calculation of the project is the second step of the HSI imager design process. Field of View (*FOV*) value across the flight direction and along the flight direction, swath width (*sw*), ground sampling distance (*GSD*), and focal length (*f*) values are calculated by the equations (1-6) before the optical design process (Shaoyuan et al.,2022, Öztürk et al. , 2023). In orbital push-broom imaging sensors, a line of on-ground pixel images arranged perpendicular to the flight direction of the spacecraft as can be seen in Figure 1. In the across flight direction, on ground smile is restricted to be the 10% of the pixel projection. The system design parameters are calculated as the following.

$$GSD = \frac{H.p}{f} \quad (1)$$

$$sw = GSD\ x\ \#sp \quad (2)$$

$$\theta_{along} = \pm tan^{-1}\left(\frac{sw}{2.H}\right) \quad (3)$$

$$\theta_{across} = tan^{-1}\left(\frac{1.5\ m}{H}\right) \quad (4)$$

$$d_{spec} = p * \#sp \quad (5)$$

$$d_{spat} = p * \ \#stp \quad (6)$$

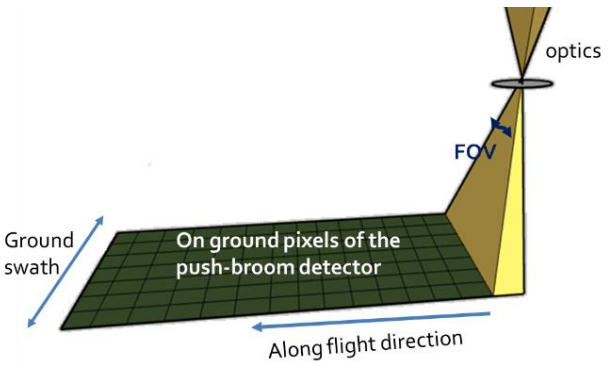

Figure 1. Scheme of the field of view (FOV) geometry and the projection of the detector array on the ground

Parameter	Symbol	Value
Ground Sampling Distance	*GSD*	≤ 15 m
Focal Length	f	712 mm
FOV along flight direction	θ_{along}	± 0.61 °
FOV across flight direction (Spectral field)	θ_{across}	1.22 10^{-4} °
Swath width	sw	15.3 km
Spectral detector width	d_{spec}	3.84 mm
Spatial detector width	d_{spat}	15.36 mm

Table 4. Calculated system parameters

4. OPTICAL SYSTEM DESIGN OF THE HYPERSPECTRAL IMAGER

Hyperspectral spaceborne imager designs comprise of two parts: telescope and spectrometer. Off-axis TMA type telescope is selected for the telescope design and modified-Offner type spectrometer is selected for the spectrometer design. In the spectrometer design two Féry prisms are used as a diffractive element. A real ray-tracing software (i.e., Zemax OpticStudio) is used to optimize the HSI.

4.1 Telescope Design

The design of a TMA telescope is more complex than other types of telescopes, but it offers several advantages, including a larger field of view, a flatter focal plane, and better image quality across

the entire field of view (FOV) (Chang et al., 2016, (Wang et al., 2022). TMA is corrected for the third-order aberrations of spherical aberration, coma, and astigmatism. Moreover, off-axis TMA design is freeform without obscuration which allows for more signal transferred towards sensor.

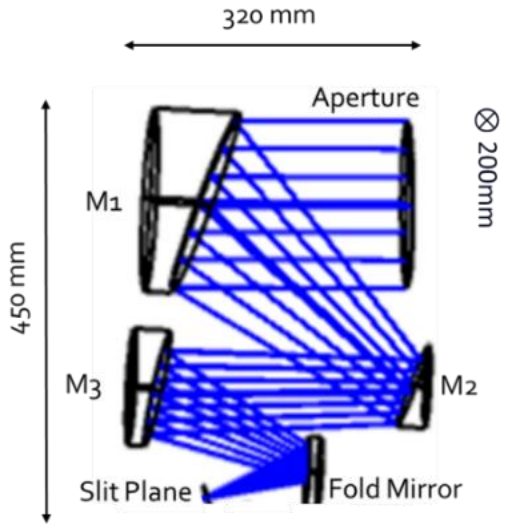

Figure 2. TMA telescope design layout of the HSI

Optimization process started with the standard aspheric surface. Maximum total length of the telescope is constrained to fit in 320 mm. However, optimization is not possible with the standard aspheric surface form with the restriction of the TMA telescope dimensions. Even aspheric surfaces are often used in the design of lenses, mirrors, and other optical components to improve their performance (Amani et al., 2020). They can help to reduce aberrations, improve image quality, and increase the efficiency of light transmission through the optical system. Even aspheric surface type is chosen to optimize the system in limited dimensions. Even aspheric surface sag equation is given by (7):

$$z(r) = \frac{cr^2}{1+\sqrt{1-(1+k)c^2r^2}} + A_2r^2 + A_4r^4 + A_6r^6 + A_8r^8 + A_{10}r^{10} \quad (7)$$

where, z is the sag equation, c (1/R) is the curvature of the mirror, k is the conic constant (in our case k = 0), r is the radial mirror coordinate, A_n are coefficients of the higher order terms. Three even aspheric surface mirrors and a folding mirror is used for the minimal design dimensions. TMA Telescope design optical layout and system parameters are shown in Figure 2 and Table 5 respectively. Optical design prescription of the TMA telescope design is given in Table 6. The image plane of the TMA telescope is the slit plane in the design shown in Figure 3. Slit length of the spatial direction (x-direction) is calculated from the multiplication of number of spatial pixels and pixel size. Spatial slit dimension equals to the spatial detector dimension. After the slit plane spectral sampling will be operated for each wavelength.

Parameter	Value
Aperture Diameter	200 mm
Effective Focal Length	712 mm
Dimensions	450 mm x 320 mm x200 mm
Mirror Surface Type	Even Asphere
Bandwidth	400-2500 nm
Slit Dimensions	15.3 mm x 15 µm
MTF @Nyquist	0.78
Nyquist Frequency	33 cycles per mm

Table 5. Off-axis TMA optical design parameters

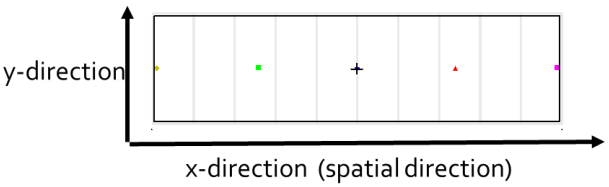

Figure 3. Footprint Diagram of the slit plane

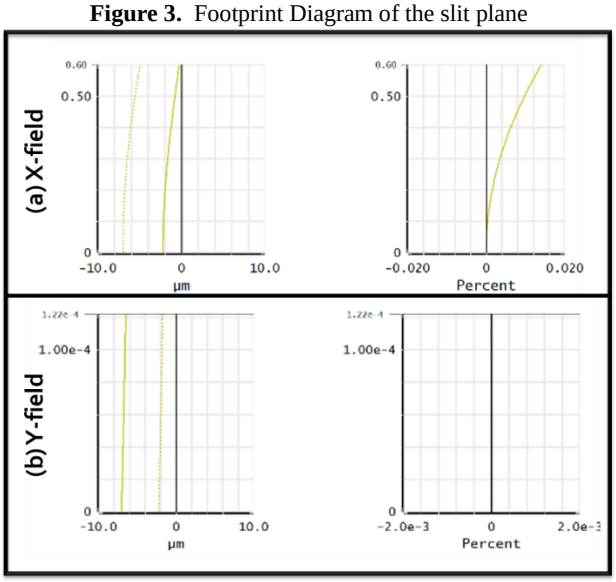

Figure 4. Field curvature and distortion results of the TMA design (a) X-field and (b) Y- field

Field curvature and distortion percentages of the TMA design for X-field and Y-field are shown in Figure 4. Field curvature values of X- and Y-field are less than 15 µm and distortion percentages are less than 0.02%. MTF of the final optimized TMA telescope is shown in Figure 5. Nyquist frequency is calculated from the eq. (8). Resulting MTF value of the designed TMA telescope at Nyquist is 0.79. Resulting Spot diagram of the TMA telescope is shown in Figure 6.

$$f_{Nyquist} = \frac{1}{2 * pixel\ size\ (mm)} \quad (8)$$

Surface	Surface Type	Radius (mm)	Thickness (mm)	Semi Diameter (mm)	Conic Constant	A_2	A_4	A_6	A_8	A_{10}
Object	Plane	-	320	100	-	-	-	-	-	-
M1	Even Aspheric	-1100.2	-300	110	0	$-6.4\ 10^{-5}$	$1.3\ 10^{-10}$	$5.2\ 10^{-17}$	$-7.7\ 10^{-23}$	$1.5\ 10^{-28}$
M2	Even Aspheric	301.9	-200	50	0	$1.2\ 10^{-4}$	$4.4\ 10^{-9}$	$1.4\ 10^{-14}$	$-2.7\ 10^{-19}$	$5.1\ 10^{-24}$
M3	Even Aspheric	-485.7	120	70	0	$1.2\ 10^{-4}$	$3.3.\ 10^{-10}$	$4.1\ 10^{-21}$	$4.4\ 10^{-27}$	$4.4\ 10^{-27}$
Image Plane	Plane	-	-	7.1	-	-	-	-	-	-

Table 6. Optical prescription of the TMA telescope design

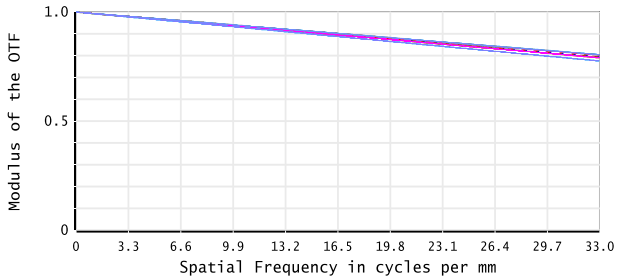

Figure 5. Resulting MTF graph of the TMA Telescope Design [400-2500 nm]

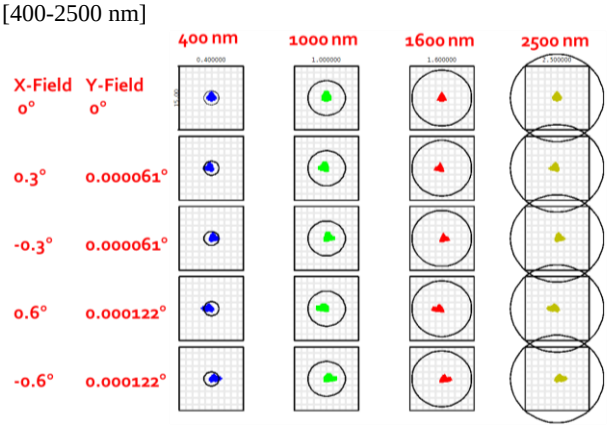

Figure 6. Resulting matrix spot diagram of the TMA telescope design (black circles represent Airy disk, black squares represent 15 µm square pixel)

Full Field Displays (FFDs) of HSI TMA design for the third-order spherical aberration, astigmatism and coma are shown (Thompson, 1985). FFDs show the field dependencies of the third-order aberrations for the full FOV.

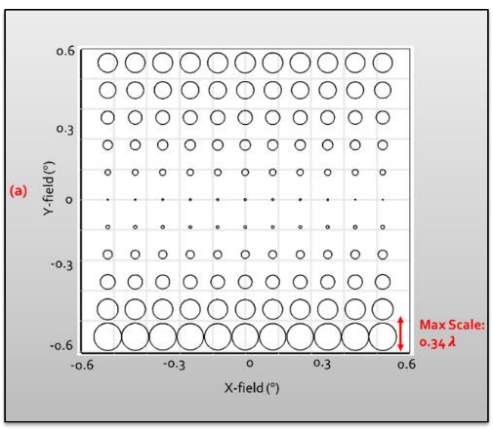

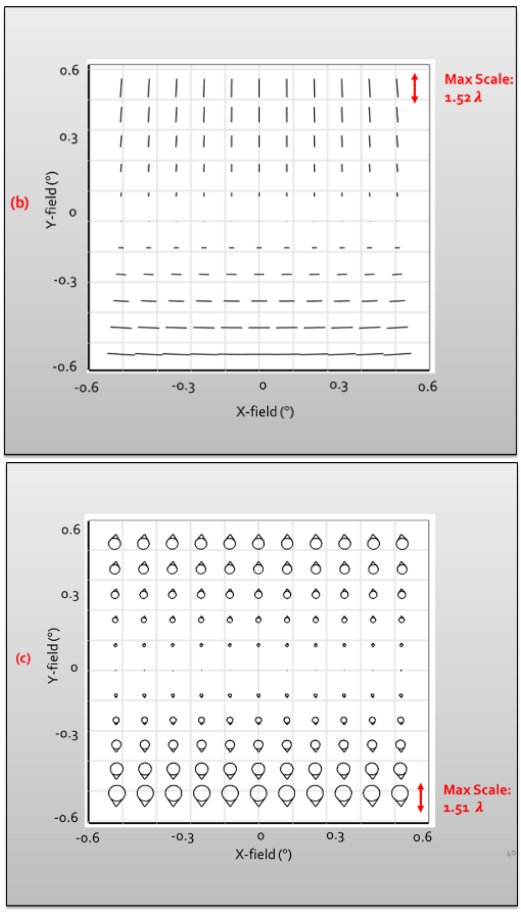

Figure 7. FFDs of the off-axis TMA for the third-order: **(a)** spherical aberration, **(b)** astigmatism, **(c)** coma

4.2 Spectrometer Design

Spectrometer design process started with the Offner type spectrometer. The Offner spectrometer was invented by Horst Offner in 1960 (Prieto-Blanco et al., 2006). It is a type of diffraction grating spectrometer, which uses a diffraction grating as a diffractive element. The grating consists of a series of closely spaced parallel lines or grooves, which diffract the light at different angles depending on the wavelength. However, Offner design with diffraction grating has low light efficiency due to the diffraction of light into its orders and does not able to optimize large FOV in a compact form. Then, Modified-Offner spectrometer with Fery prism is used, which was invented by C. Féry in 1911 (Nie et al., 2018). The difference between

traditional prism and Féry prism is the change in the surfaces of prism. Féry prism has spherical type of surfaces instead of plane surface that can focus the spectral image on the detector plane effectively.

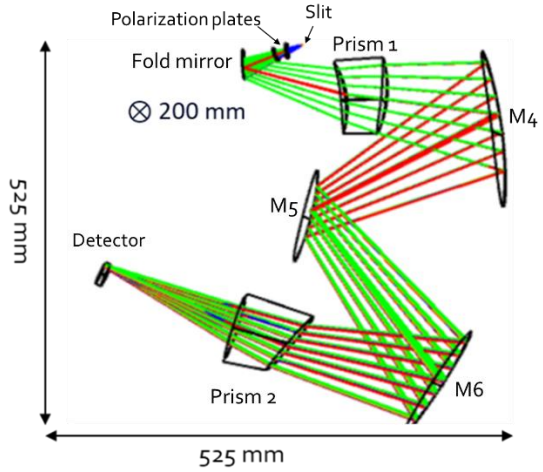

Figure 8. Design layout of the HSI spectrometer

Parameter	Value
Dimensions	525 mm x 525 mm x 200 mm
Mirror Surface Type	Even Aspheric
Bandwidth	400-2500 nm
Prism type	Fery
Prism Material	CaF2
Polarization Plate Material	Silica
Average Spectral Sampling	8 nm
Detector vacuum window material	Silica

Table 7. Spectrometer specifications

Parameter	M4	M5	M6
Radius (mm)	488.4	-323.3	488.4
A_2	-6.9 10^{-5}	1.5 10^{-4}	-6.9 10^{-5}
A_4	-8.9 10^{-11}	4.2 10^{-9}	-8.9 10^{-11}
A_6	-3.6 10^{-16}	3.9 10^{-14}	-3.6 10^{-16}
A_8	-3.7 10^{-22}	2.8 10^{-18}	-3.7 10^{-22}

Table 8. Spectrometer mirror specifications

Parameter	Prism 1	Prism 2
Radius front (mm)	106.4	386.4
Radius back (mm)	136.1	286.1
Thickness (mm)	32	25
Apex angle (°)	13	24

Table 7. Spectrometer prism specifications

Spectrometer part starts with the slit. After the slit, there are two flat polarization plates aiming to make hyperspectral design equally sensitive for both s-polarized and p-polarized light. These plates are placed under opposite angles with the optical axis and positioned between the slit and the folding mirror. In the HSI spectrometer design three concentric even aspheric surface type mirrors are used. Likewise, the Offner kind of mirror configuration three mirrors share the same optical center M4 and M6 mirrors are the same mirrors as can be seen from Table 8 (Nie et al., 2018). To reduce the weight of the imager modified-Offner spectrometer mirror is divided into two mirrors in the design and the unused region of the mirror is subtracted from the design. Moreover, two Féry prisms are preferred as a diffractive element in the design. Specifications of the prisms are shown in Table 8. A folding mirror is used to make the spectrometer fit in the limited dimensions. Finally, detector is designed to be in a vacuum box with a window defined in the design. This vacuum window makes the detector operate in low temperature conditions. Spectrometer part of the HSI design optical layout is shown in Figure 8. Spectrometer specifications are given in Table 7.

5. ANALYSIS AND RESULTS

Overall HSI design is shown in Figure 9. MTF requirement of the study is 0.36. Minimum overall resulting system MTF at Nyquist frequency is 0.47 as shown in Figure 10 for 2500 nm. Best overall resulting system MTF at Nyquist frequency is 0.72 for 400 nm, shown in Figure 11. Nyquist frequency value for 15 µm detector pixel is calculated to be 33.

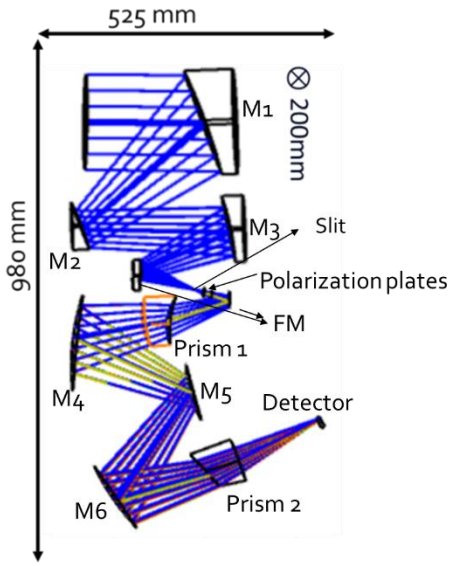

Figure 9. Overall HSI optical design layout

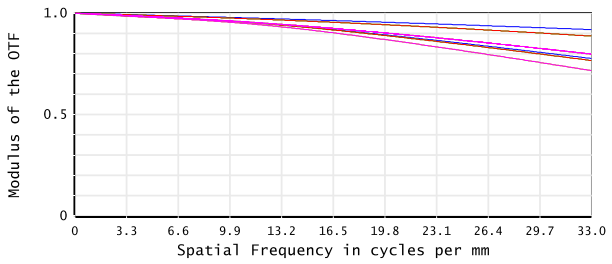

Figure 10. Resulting MTF graph of the overall HSI for 400 nm

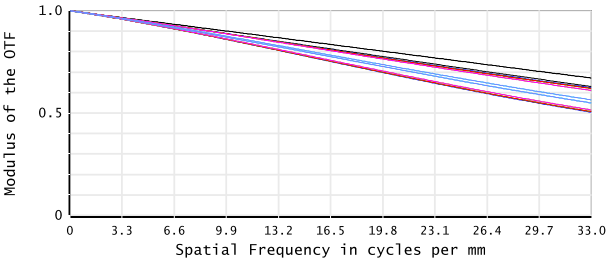

Figure 11. Resulting MTF graph of the overall HSI for 2500 nm

Field curvature and distortion values are shown in Figure 12 and Table 10, which meet the project performance goal requirements.

Smile and keystone distortion values are calculated from the spot diagram. Change in the spatial direction image width results in keystone distortion, while change in spectral direction image width results in smile distortion as can be seen in Figure 13.

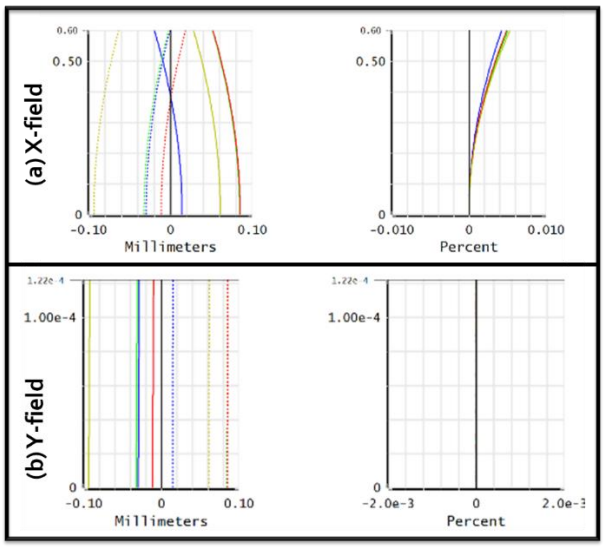

Figure 12. Field curvature and distortion results of the overall HSI design

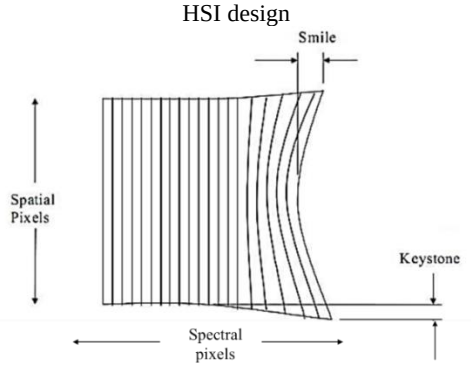

Figure 13. Keystone and smile distortion

Field Angle (°)	Smile Distortion		Keystone Distortion
	400 nm	2500 nm	
±0.3	1.98 mm	2.01 mm	2.6 mm
±0.6	8.17 mm	8.98 mm	5.3 mm

Table 8. Keystone and smile distortion results

Average spectral sampling is calculated from the total bandwidth divided by total number of spectral pixels. Average spectral sampling is calculated as 8 nm. Dimensions of the detector is calculated from total spectral and spatial number of pixels with pixel size. Spectrometer spatial magnification equals to one to avoid distortions. Moreover, spectrometer spectral sampling is tuned by the angles of the prisms and the HSI imager is optimized to fit in the spectral dimension of the detector as can be seen in Figure 14.

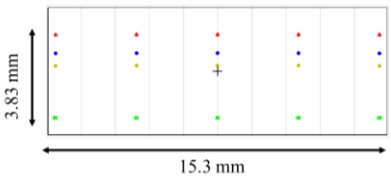

Figure 14. Footprint Diagram of the image plane

Spot diagram of the overall HSI design is shown in Figure 15. The overall HSI design is concluded to be in the diffraction limited performance.

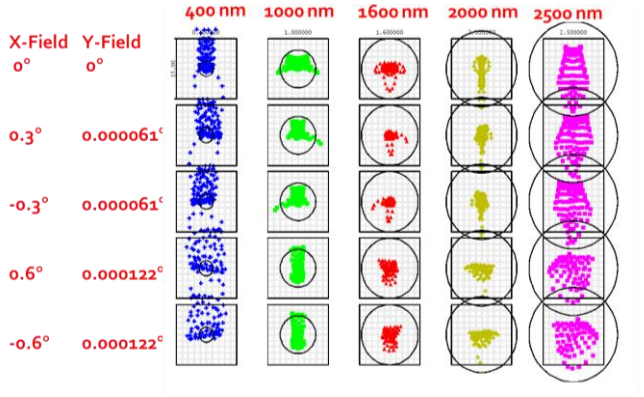

Figure 15. Spot diagram of the overall HSI design (Black circles represent Airy disk, black squares represent 15 µm square pixel)

6. CONCLUSION

In conclusion, an overall HSI design is developed and presented in this work. Off-axis TMA telescope with even aspheric mirror surface forms has been designed. This type of design avoids obscuration and satisfies the required full FOV value of 1.2 degrees with 14.7 m resolution and 15.3 km swath width. Overall optical design is corrected for the third-order spherical aberration, astigmatism, and coma. The minimum MTF value of the design is calculated to be 0.49 at Nyquist frequency. Spot diagrams show that resulting spots on the detector plane satisfies the Rayleigh criteria on each pixel of the detector. Keystone and smile distortion values are less than 15 µm requirement. Modified-Offner type spectrometer design with Féry prisms and three even aspheric form mirrors has been designed such a way that they share the same optical centre works between 400 to 2500 nm. The resulting average spectral resolution of 8.3 nm. Compactness of the design is also considered; the overall optical system can fit in a box with dimensions 980 mm x 525 mm x 200 mm (Volume of the design= 0.1 m^3). The HSI design is concluded to meet the performance goals of the project which aims to be used in monitoring of Earth's surface for environmental purposes operating in LEO. Hyperspectral design is planned to be realized micro-satellite platforms in near future.

7. REFERENCES

Amani A., Bai J., Huang X., 2020. Dual-view catadioptric panoramic system based on even aspheric elements. *Applied Optics*, 59(25), pp. 7630-7637.

Bergeron M., Hollinger A., Staenz K., Maszkiewicz M., Neville R.A., Qian S.-E., Goodenough D. G., 2008. Hyperspectral Environment and Resource Observer (HERO) mission. *Can. J. Remote Sensing*, p. S1–S11.

Calin M. A., Calin C. A. , Nicolae D. N. , 2021. Application of airborne and spaceborne hyperspectral imaging techniques for

atmospheric research: past, present, and future. *Applied Spectroscopy Reviews,* Volume 56, pp. 289-323.

Chang S. T. ,Lin Y. C. , Wu K.H. ,Lien C.C. , Huang T. M., Tsay H. L., Chan C.Y., 2016. *The design and assembly of aluminum mirrors of a three-mirror-anastigmat telescope.* Biarritz, Proceedings of the SPIE, pp. 1-6.

Eismann, M. T., 2012. *Hyperspectral Remote Sensing.* Washington: SPIE Press.

Escalante-Ramírez, B., 2012. *Remote Sensing Advanced Techniques and Platfroms.* Croatia : InTech .

K. P. Thompson, 1985. *Beyond optical design Interaction between the lens designer and the real world.* s.l., SPIE Proceedings, pp. 426-438.

M. Celesti, M. Celesti, J. Adams, V. Boccia, F. Gascon, C. Isola, J. Nieke, 2022. The Copernicus Hyperspectral Imaging Mission for the Environment (CHIME): Status and Planning. *IEEE International Geoscience and Remote Sensing Symposium,* pp. 5011 -5014.

Nie Y., Zhang J., Wang J., Xiang L., 2018. Optical design and performance comparison of various hyperspectral imagers based on Fery prisms. *Journal of Advanced Optics and Photonics,* 1(4), pp. 279-290.

Öztürk Z. N., Başlar İ., Selimoğlu Ö., Karcı Ö., 2023. Signal-to-noise ratio model in Python for high-resolution space-borne electro-optic imagers. *SPIE JARS,* 17(1), pp. 1-18.

Qian, S.-E., 2021. Hyperspectral Satellites Evolution and Development History. *IEEE JARS,* Volume 14, pp. 7032-7056.

Shaoyuan, C., 2022. *Geometric parameters analysis of two large FOV space-borne optical.* Beijing, Proc. SPIE , pp. 1-6.

Wang J., He X., Zhang X., Ma M., Cao Z., 2022. Wave Aberration Correction for an Unobscured Off-Axis Three-Mirror Astronomical Telescope Using an Aberration Field Compensation Mechanism. *MPDI Appl. Sci. ,* 12(21), p. 10716.

X. Prieto-Blanco, C. Montero-Orille, B. Couce, R. de la Fuente, 2006. Analytical Design of an Offner Imaging Spectrometer. *Optics Express,* 14(20), pp. 9156-9168.